CHAPTER 5

MODEL TESTS ON EMBANKMENT

5.1 General

Granular columns have been used widely over the years to improve the load-bearing capacity of soft soils. Conventional granular columns are composed of stone aggregates, a non-renewable natural resource. Meanwhile, the global stockpile of plastic waste poses another serious threat to the sustainable existence of lives on our planet. This paper highlights the results of laboratory model tests performed on an embankment supported over a soft clay bed improved with granular columns (GC) and plastic granular columns (PGC). The model embankment was subjected to static and cyclic loading tests. The cyclic loading was applied in a 4-stage varying amplitude and single-stage loading.

In the present study, a model embankment was constructed over a soft clay bed to simulate embankments for transportation routes. The soft cay bed underlying the model embankment was reinforced with Granular columns (GC) and plastic granular columns (PGC). Stone aggregates were used for GC, and recycled waste plastic granules were used in PGC. The granular columns were encased to act as encased granular columns (EGC) and encased plastic granular columns (EPGC).

This study's prime objective is to use recycled waste plastic granules as a sustainable alternative to conventional stone aggregates. Twelve columns of 40 mm diameter were installed in a rectangular group pattern. The columns were installed in floating and end-bearing column configurations. Strain-controlled static loading was performed on the model embankment. Four-stage and single-stage cyclic loading tests

were performed on the improved bed. This paper presents the results of the laboratory model tests done under static and cyclic loading. It presents the response of embankment in terms of vertical settlement, excess pore water pressure (EPWP), and stress concentration ratio (n). EPWP in the soil mass was measured using a pore pressure transducer, and stresses on the column and neighboring soil mass were evaluated with the help of earth pressure cells. Using granular columns composed of plastic granules has numerous practical applications, including developing large logistics parks, oil storage facilities, railway and highway embankments, and runways. They also enhance the bearing capacity of areas underlain by soft soil deposits**.**

5.2 Experimental program

This study discusses laboratory tests on an embankment model constructed over soft clay beds reinforced with GC and PGC. The columns were installed in a rectangular group pattern. Sixteen lab tests were conducted on the model test embankments constructed on unreinforced and granular column-reinforced clay beds. Three tests were performed on unreinforced, GC-reinforced clay beds with floating and end-bearing columns subjected to static (strain-controlled) loading. The scheme of the laboratory model tests with the adopted parameters is shown in Table 5.1. Nine multistage cyclic loading tests were performed on GC, PGC, EGC, and EPGC-reinforced clay beds supporting soil embankments. Four single stage cyclic loading tests were also performed on model embankment.

Table 5.1 Summary of the model tests performed.

Test series	Type of soil reinforcement	Length, l (mm)	Column configuration	Type of loading
1	UR			Static
2	UR			Cyclic
3	GC	320	Floating	Static
4	GC	400	End bearing	Static
5	GC	320	Floating	Cyclic
6	GC	400	End bearing	Cyclic
7	PGC	320	Floating	Cyclic
8	PGC	400	End Bearing	Cyclic
9	EGC	320	Floating	Cyclic
10	EGC	400	End bearing	Cyclic
11	EPGC	320	Floating	Cyclic
12	EPGC	400	End bearing	Cyclic
13	GC	400	End bearing	Cyclic (Single stage)
14	PGC	400	End bearing	Cyclic (Single stage)
15	EGC	400	End bearing	Cyclic (Single stage)
16	EPGC	400	End bearing	Cyclic (Single stage)

Note: UR= Unreinforced soil; l=length of the granular column.

Static load tests were performed in strain-controlled mode on an unreinforced soil bed and GC (end-bearing and floating) reinforced clay bed. The granular columns had a 40 mm diameter, and two different lengths, 320 mm and 400 mm, were used in the model tests. The arrangement of the model tests along with the instruments used in the study are illustrated in Fig. 5.1.

Cyclic loading was applied in a load-controlled mode in a sinusoidal (only compression) waveform to simulate the cyclic loading of a railway embankment. The cyclic stress induced by the movement of trains over railway tracks was taken into consideration for the evaluation of the dynamic behavior of railway embankments in this study. The estimated cyclic stress on the railway embankment is calculated using the empirical equation proposed by Ashour (Ashour et al. 2022).

Fig. 5.1 Systematic representation of model test setup, sensors and data acquisition system.

5.3 Results and discussion

5.3.1 Static load testing

Static strain-controlled load tests were performed on a model embankment supported by an underlain soft clay bed. In this study, the vertical stress experienced by the model embankment at 50 mm of settlement is considered the peak stress for each soil sample during all loading tests.

5.3.1.1 Deformation behavior under static loading

The results of the static loading tests conducted on the model embankment constructed over a soft clay bed are shown in Fig. 5.2. Static loading tests were also performed on the model embankment resting over a reinforced clay bed in the floating and end-bearing configuration. The results present a comparative analysis of the load settlement behavior of the GC-reinforced bed over the unreinforced soil bed. It could be observed from the stress settlement plot shown in Fig. 5.2 that the presence of a reinforced clay bed under the embankment significantly improves its vertical loading capacity. The model test results show higher improvement for end-bearing GC improved clay bed; this could be attributed to the mobilized higher stiffness of the composite clay bed. The vertical stress acting on the embankment increased with its settlement in the downward direction. The vertical stress intensity at 50 mm settlement is reported as the ultimate or peak loading intensity of the embankment; this was decided based on the vertical displacement limitation of the loading actuator used in the tests. The peak stress intensity of the unreinforced soil bed was 38 kPa. The peak loading capacity of the GC-reinforced clay bed was 65 kPa for the floating columns configuration and 81.26 kPa for the end-bearing columns condition. The soil bed improved with floating columns exhibited a 71 % increase in the stress-bearing capacity, and the end-bearing column-supported soil bed exhibited a 113.5 % improvement. These results conform well with the findings of existing research works (Nishant and Kumar 2024).

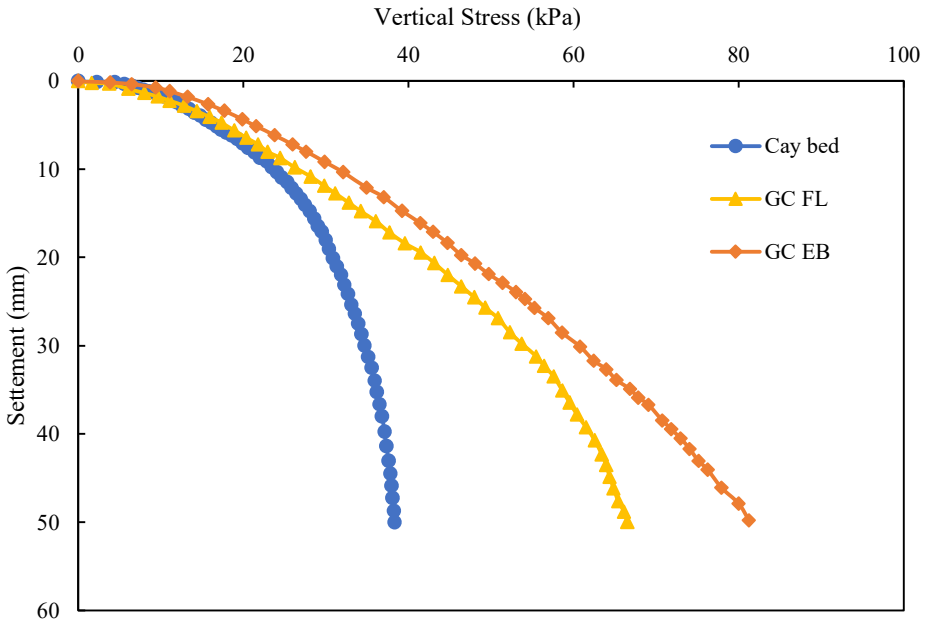

Fig. 5.2 Load settlement behavior of model embankment on soft clay bed and bed reinforced bed with GC under static loading.

5.3.1.2 Excess pore pressure variation under static loading

This section presents the variation of excess pore water pressure and stress concentration in response to static loading of the model embankment constructed over a soft clay bed. The results of the static loading tests done on model embankment over unreinforced and GC-reinforced clay beds are shown in Fig. 5.3. The excess pore pressure plot was found to follow an increasing trend with the increase in vertical deformation with peak pore pressure of 5.93 kPa at 50 mm settlement. The excess pore pressure distribution for the soil bed reinforced with GC in floating and end-bearing conditions has also been presented here. It was observed that the presence of granular columns helps reduce the maximum excess pore pressure induced in the soil mass due to static load loading. The reduction in excess pore pressure was more significant for end-bearing GC. The peak excess pore pressure is 2.87 kPa for end-bearing GC and 4.90 kPa for floating GC.

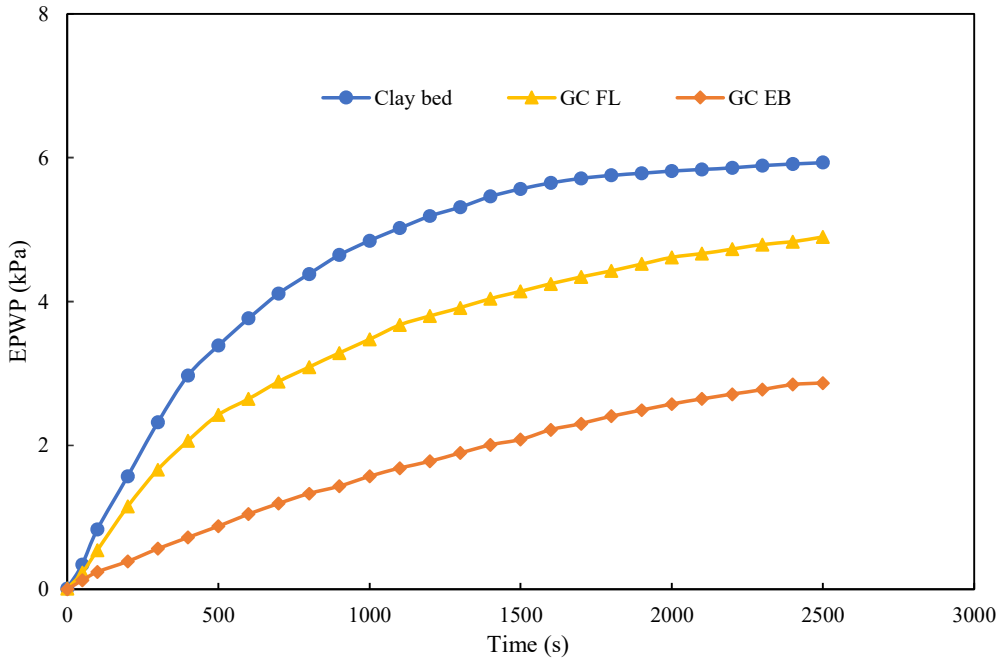

Fig. 5.3 Excess pore water pressure variation for soft clay bed and bed reinforced with GC under static loading.

5.3.1.3 stress concentration ratio (n) variation under static loading

The presence of GC reinforcements in the soft clay bed helps reduce the stress in the soil mass as a higher load is borne by the granular column than the surrounding soil. The stress induced on the GC and the surrounding soil was measured using earth pressure sensors. The stresses measured using these sensors are presented in terms of stress concentration ratio (n), defined as the ratio of the stress on the granular column to the stress on the neighboring soil (Ghazavi and Nazari Afshar 2013). Fig. 5.4 shows the variation of n for end-bearing and floating GC with the increase in embankment settlement under the action of load. As seen in the graph, 'n' is found to quickly increase with the vertical settlement reaching a peak and gradually decreasing to attain a steady state consistent with previous studies (Ghazavi and Nazari Afshar 2013; Pradeep et al. 2024). This observation could be attributed to the initial densification of the column material and the gradual transfer of load to the surrounding soil. The peak value of n

was found to be 7.54 for end-bearing GC and 5.90 for floating GC. A higher *n* value for end-bearing column supported embankment indicates that higher stresses are borne by end-bearing column configuration. The stress concentration ratio reaches an approximately stable value of 1.92 and 1.54 for the end-bearing and floating GC after 2000 seconds of loading.

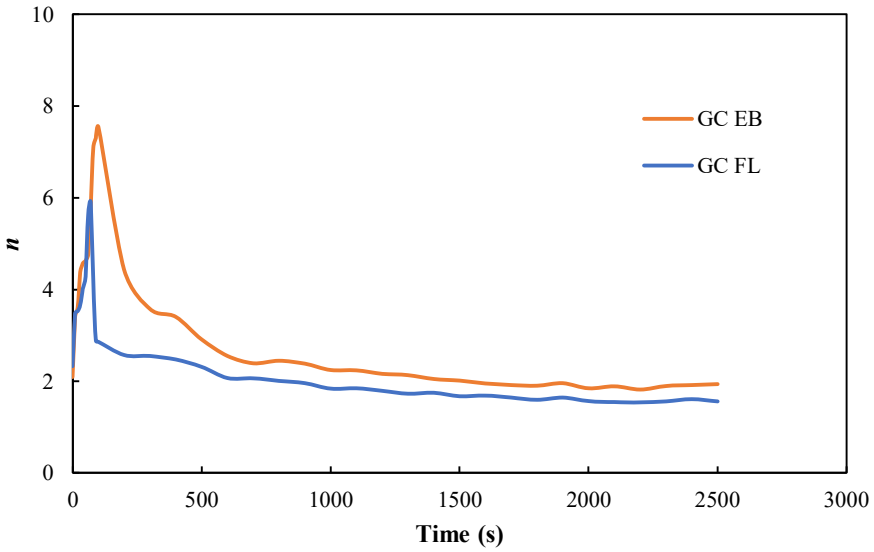

Fig. 5.4 Variation of stress concentration ratio (n) for GC-supported embankments under static loading.

5.3.2 Cyclic loading response of model embankment

Stress controlled cyclic loading tests were performed on an embankment supported by granular column reinforced soft clay bed. The loading of the model was done in accordance with the scheme and the type of tests mentioned earlier.

5.3.2.1 Cyclic load vs. settlement response of the embankment

Staged cyclic loading tests were conducted on a model embankment constructed over an unreinforced and improved clay bed. The clay bed was improved using a group of GC and PGC under floating and end-bearing column configurations. The vertical stress-settlement response of the model tests conducted under cyclic loading is shown

in Fig. 5.5. The settlement of the embankment surface is observed to increase rapidly at first, then a gradual decrease in the rate of accumulated settlement occurs. The variation of footing settlement with the number of loading cycles is nonlinear for stage 1 of the loading. Cumulative settlement occurs with further application of stage 2 and stage 3 cyclic loads. An increased settlement rate is observed with a steep accumulation of footing settlement for subsequent stages. The cyclic settlement response of embankment agrees well with results reported by other cyclic loading studies (Xu et al. 2024). The settlement trend of floating columns reinforced clay bed is similar to that of the end-bearing columns, but the settlement rate is higher. The comparative response of an unreinforced clay bed under cyclic load is also depicted in Fig. 5.5. The embankment constructed on an unreinforced clay bed exhibited a 50 mm settlement within 662 cycles of loading.

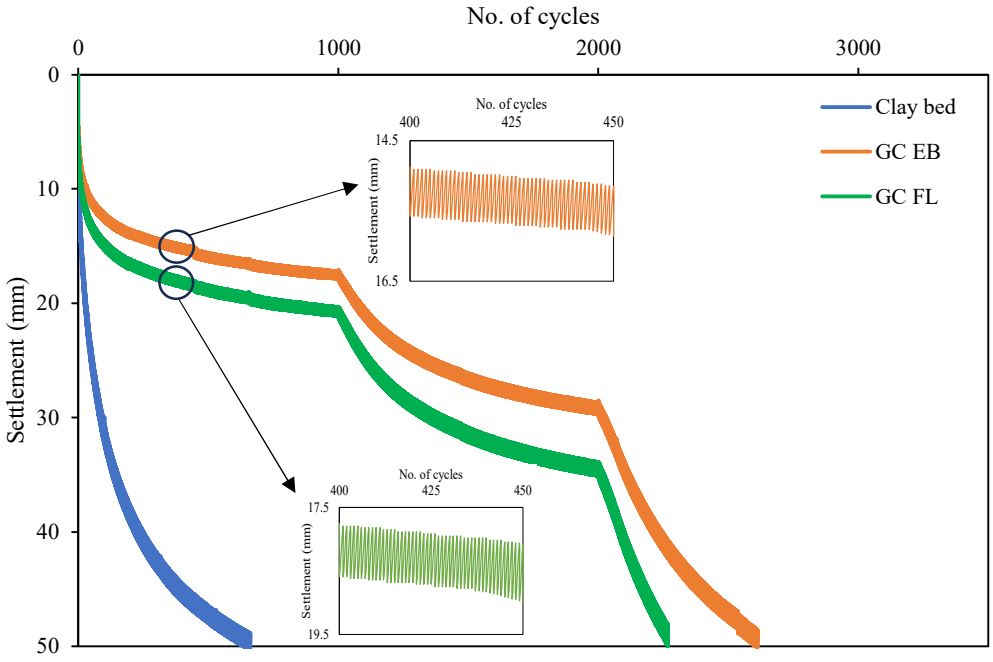

Fig. 5.5 Cyclic load induced settlements of footing in unreinforced and GC-reinforced soil bed with multiple stage load cycles.

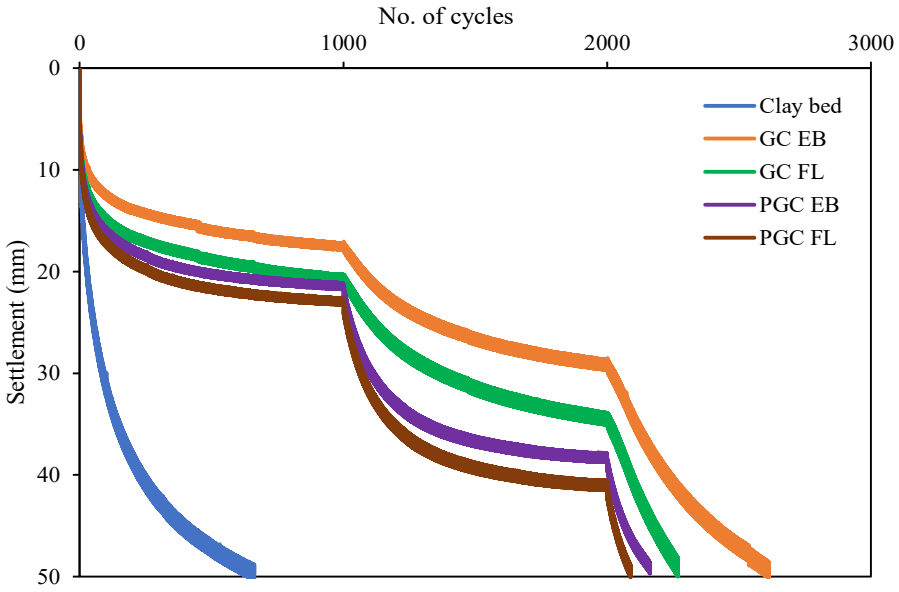
No. of cycles
0
1000
2000
3000
0
10
20
30
40
50
Settlement (mm)
Clay bed
GC EB
GC FL
PGC EB
PGC FL

(a)

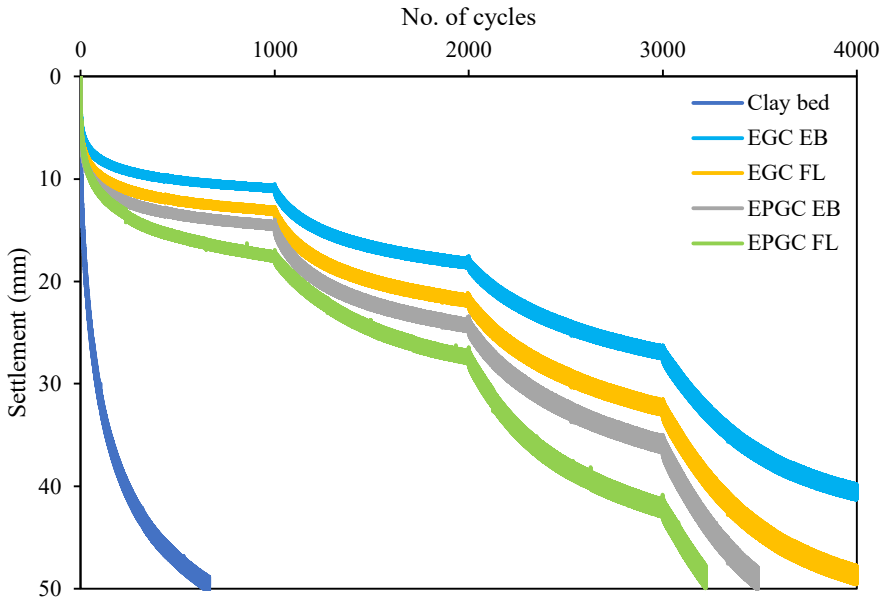
No. of cycles
0
1000
2000
3000
4000
0
10
20
30
40
50
Settlement (mm)
Clay bed
EGC EB
EGC FL
EPGC EB
EPGC FL

(b)

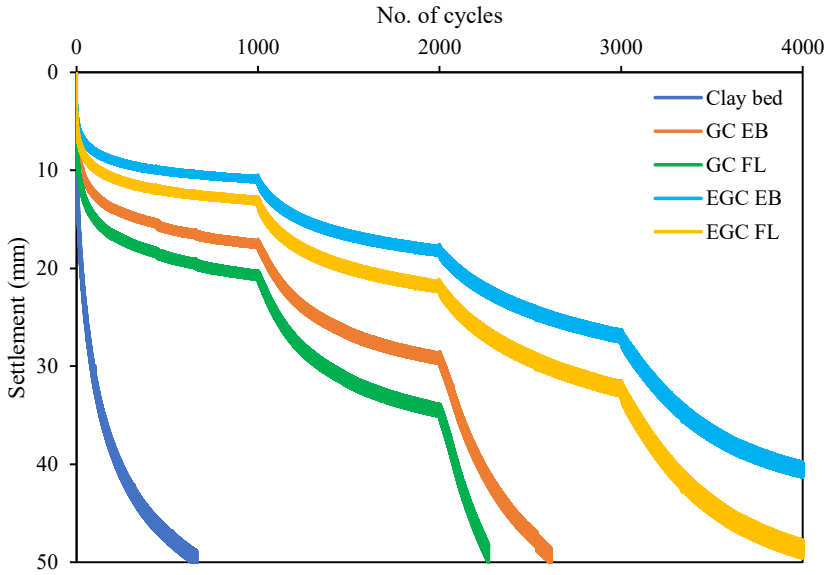

(c)

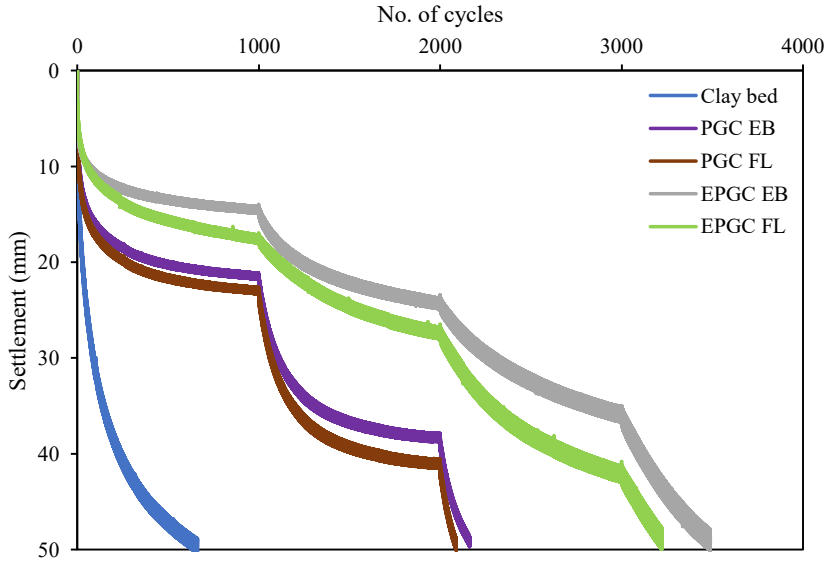

(d)

Fig. 5.6 Settlement response embankment over unreinforced and reinforced clay bed under 4-stage cyclic loading with column configurations; (a) GC and PGC; (b) EGC and EPGC; (c) GC and EGC; and (d) PGC and EPGC.

Note: GC EB= End-bearing granular columns; GC FL= Floating granular columns; PGC EB= End-bearing plastic granular columns; PGC FL= Floating plastic granular

columns; EGC EB= End-bearing encased granular columns; EGC FL= Floating encased granular columns; EPGC EB= End-bearing encased plastic granular columns; EPGC FL= Floating encased plastic granular columns

Fig. 5.6 shows the effect of column length, column material, and geosynthetic encasement of columns on the cyclic loading response of the model embankment. The settlement response of unreinforced clay bed, GC, and PGC is shown in Fig. 5.6 (a). It could be observed that using granular columns in the soft clay bed drastically improves the cyclic response of the embankment. Higher settlement is observed in each stage of loading for floating columns than for end-bearing columns. At 600 cycles of loading, the settlement of the unreinforced clay bed at 49.54 mm is reduced to 22.42, 20.94, 19.73, and 16.69 for PGC Fl, PGC EB, GC FL, and GC EB, respectively. The corresponding reduction in the settlement is 54.75 %, 57.74 %, 60.18 %, and 66.31 %. The effect of geosynthetic encasement of the column on the cyclic behavior of the embankment is shown for both EGC and EPGC in Fig. 5.6 (b). The accumulated settlement of the model embankment was restricted to 41.3 mm at the end of 4000 cycles for end-bearing EGC. In contrast, the settlement reaches 50 mm for EPGC at just 3488 loading cycles. Higher settlement was observed for the floating columns case, even when geosynthetic encasement was used. The geosynthetic encasement improves the cyclic loading response significantly for both EGC and EPGC-improved clay beds. Fig. 5.6 (c) and (d) present the comparative cyclic response of GC-EGC and PGC-EPGC cases of reinforcement. A significant upgrading of the settlement plot is seen for the encased column improved bed in both the cases of GC and PGC, thus highlighting that EPGC can be on par with GC and floating EGC.

5.3.2.2 Variation of excess pore water pressure (EPWP)

A nonlinear response was observed for the excess pore water pressure with an increasing number of load cycles, as shown in Fig. 12. The EPWP increases rapidly up to 2.51 kPa at 50 mm settlement for the unreinforced clay bed. The peak of the EPWP plot is observed at the end of the cyclic loading stages. The presence of GC and PGC reinforcement results in a relative reduction of EPWP through all the stages of cyclic loading. The EPWP in the unreinforced cay bed at the end of 600 load cycles was found to be 2.35 kPa; this value of EPWP is reduced to 1.57 kPa for PGC FL, 1.21 for GC FL and 0.60 for EGC FL as seen in Fig. 5.7 (a) and (b). The reduction in EPWP could be due to the sharing of stresses by the columns. The stresses borne by the soil mass are reduced, thus lowering development of EPWP. Also, granular columns act as vertical drains in the soil mass, which helps with EPWP dissipation. The wide gap in the EPWP plot in Fig. 5.7 (b) and (c) highlights the significance of geosynthetic encasement of GC and PGC for higher EPWP dissipation. The plot trend is increasing throughout, but the provision of encasement material flattens the curve as each stage progresses.

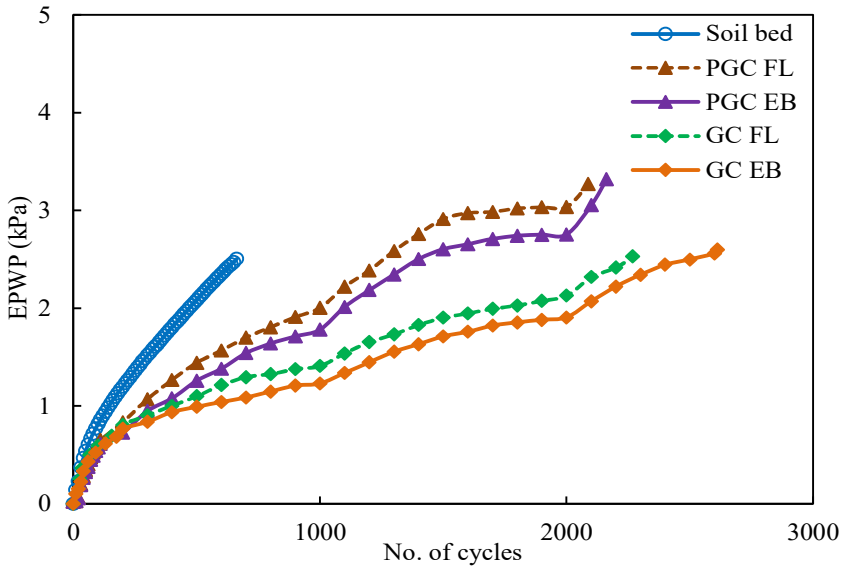

(a)

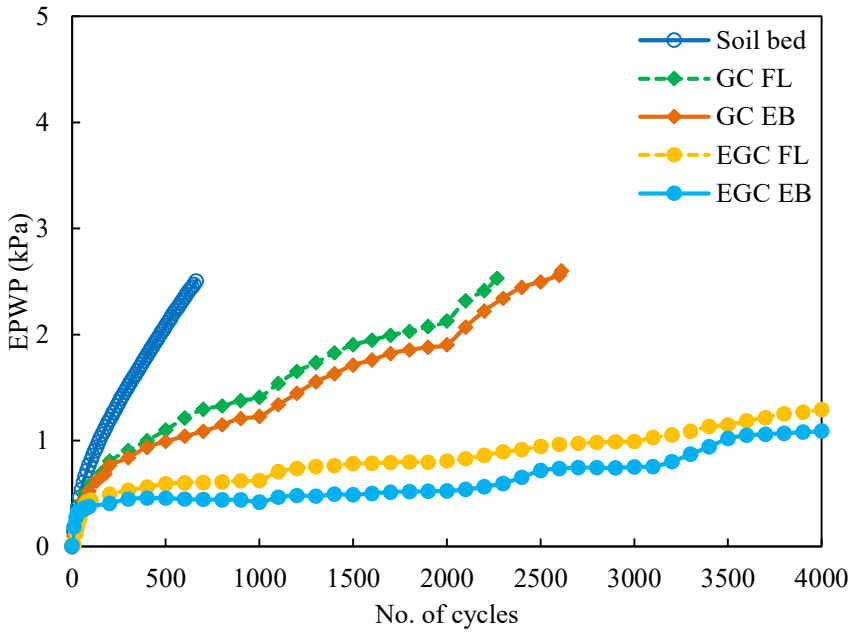

(b)

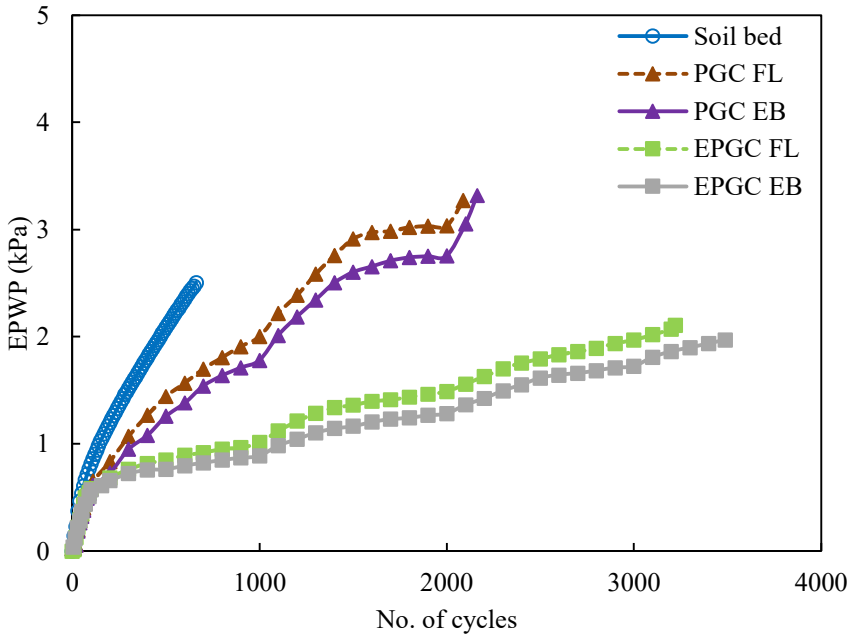

(c)

Fig. 5.7 Variation of excess pore water pressure under cyclic loading for floating and end-bearing cases: (a) GC and PGC; (b) GC and EGC; and (c) PGC and EPGC.

5.3.2.3 Variation of stress concentration ratio (n)

The stress concentration ratio for the model embankment changes with the number of loading cycles; this is shown in Fig. 5.8. The stress concentration ratio shows a sharp rise in the early loading cycles, which decreases gradually and tends to stabilize at the end of each stage. Since n is calculated as a ratio of stress on the column to that on the surrounding soil, a higher n indicates that more significant stress is shared by the granular column. Fig. 5.8 (a) shows that the n vs. loading cycles plot forms a downward-stepping trend. Since the cyclic stress amplitude increases for every successive loading stage, the soil and the column stress increases. The effective increase in stress on the soil is higher, thus the reason for the observed trend. The presence of geosynthetic encasement causes the columns to share higher stresses in subsequent loading; as such, an upward-stepping trend of variation is observed in EGC and EPGC-improved cay beds. The magnitude of n varies from 3.66 to 3.88 for EGC FL and 2.90 to 2.18 for GC FL.

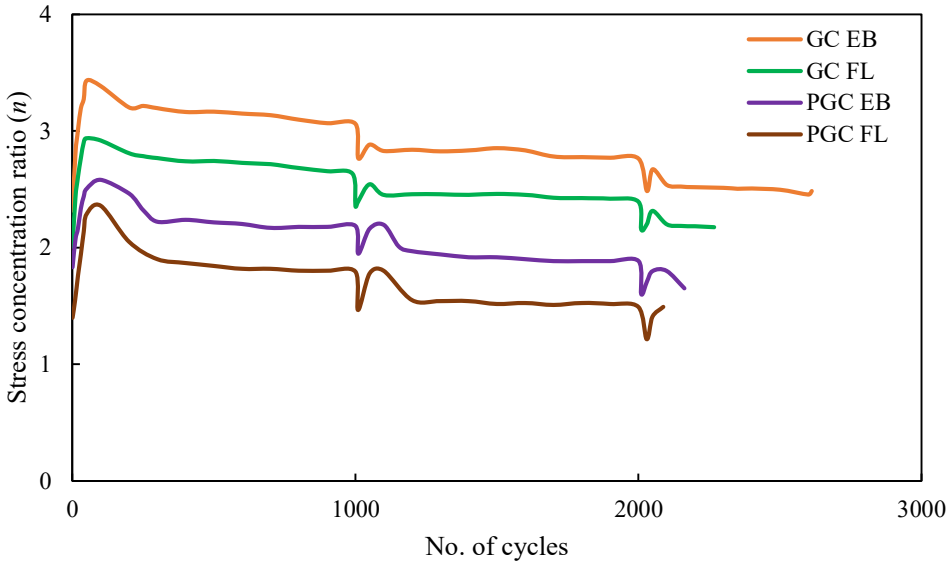

(a)

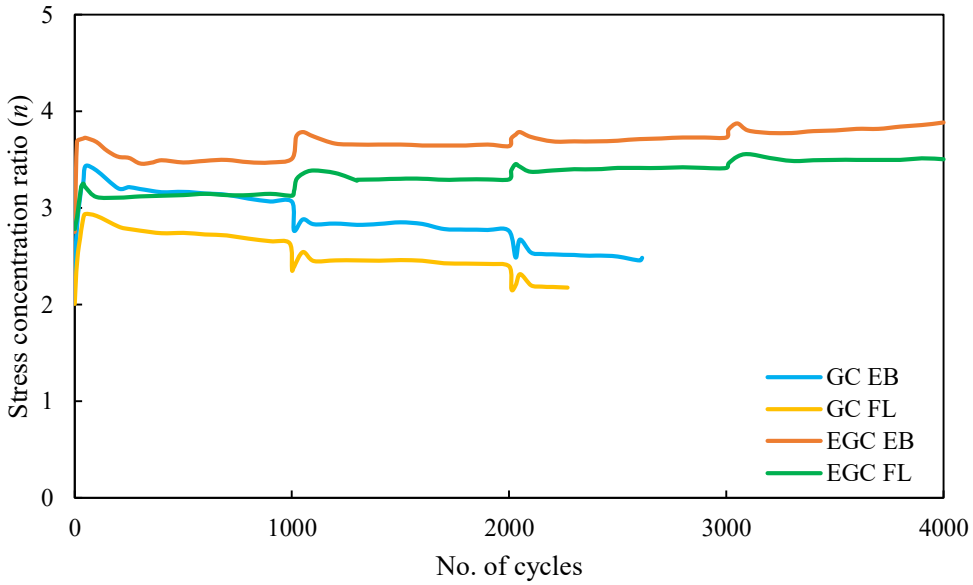

(b)

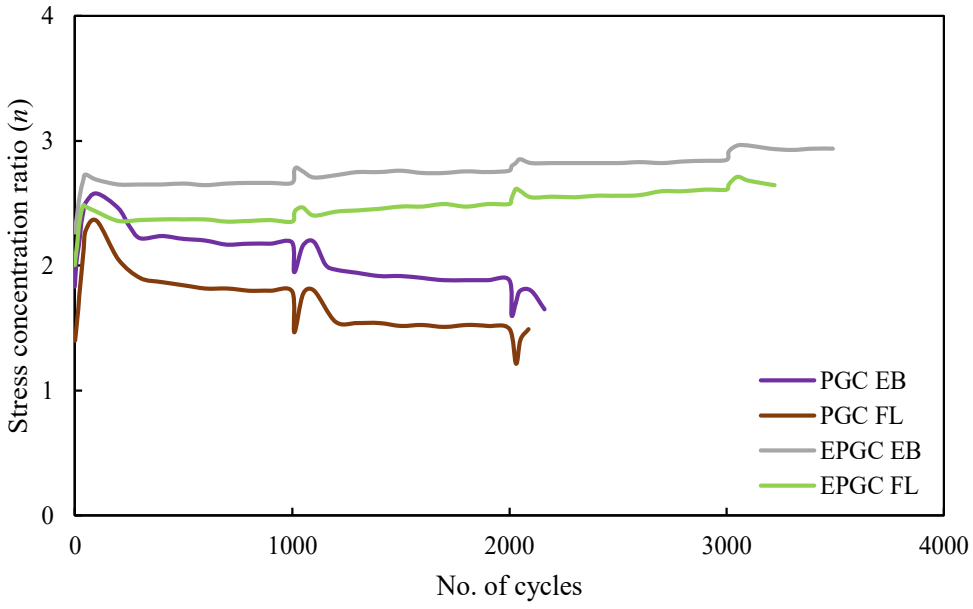

(c)

Fig. 5.8 Variation of stress concentration ratio (n) under cyclic loading for floating and end-bearing cases: (a) GC and PGC; (b) GC and EGC; and (c) PGC and EPGC.

From Fig. 5.8 (b), GC EB and EGC FL show similar n variation trends for stage 1 loading, indicating that end-bearing GC is on par with floating EGC at lower stress intensities. The upward stepping trend on *n* for encased columns was observed because the EGC bears higher stresses during loading. Upon successive loading stages, the incremental growth in stress is higher for end-bearing columns. A summary of the *n* values obtained from the test results has been presented in Table 5.2.

Table 5.2 Summary of the stress concentration ratio (n) for the multistage cyclic model

Test	Stress concentration ratio (*n*)			
	Stage 1	Stage 2	Stage 3	Stage 4
GC EB	3.25	2.88	2.64	-
GC FL	2.90	2.54	2.31	-
PGC EB	2.56	2.17	1.80	-
PGC FL	2.31	1.76	1.49	-
EGC EB	3.71	3.75	3.78	3.82
EGC FL	3.25	3.36	3.45	3.56
EPGC EB	2.72	2.77	2.85	2.98
EPGC FL	2.47	2.49	2.56	2.71

5.3.3 Effect of single-stage cyclic loading

The results obtained in the 12 model tests performed in the laboratory clearly illustrate that end-bearing granular columns perform better than floating columns under static and cyclic loading. Test series number 13 to 16 stated in the experimental program Tabe 5.1 were performed to study the response of model embankment constructed over reinforced clay bed subjected to a single stage higher cyclic stress (stage 4 stress) amplitude from beginning to the failure condition and compare it with the results of the

multistage cyclic loading tests performed in the previous sections. The single-stage settlement response of the end-bearing EGC, EPGC, GC, and PGC reinforced cay bed is depicted through the plots in Fig. 5.9. It can be observed that non-encased PGC and GC-supported embankments undergo rapid settlements reaching 50 mm vertical settlements within 165 cycles and 308 cycles respectively. Columns encased with geosynthetics have exhibited higher settlement resistance, with EPGC taking 1440 cycles and EGC taking 3000 cycles of loading to reach 50 mm vertical settlement. The stress concentration ratio shows an increasing trend initially, which peaks after a few cycles and then reaches a stable value, as shown in Fig. 5.10.

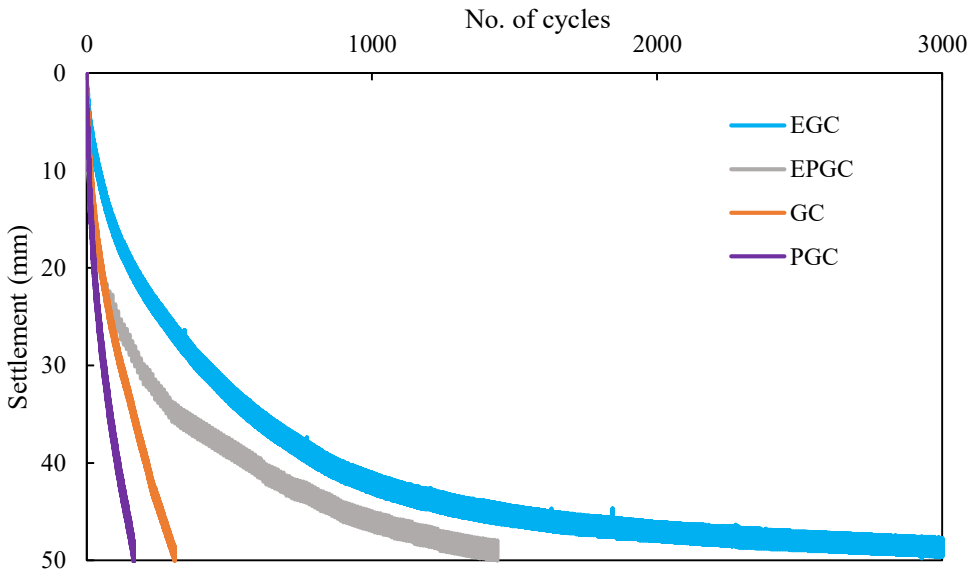

Fig. 5.9 Settlement response of single-stage (stage 4) cyclic loading on model embankment.

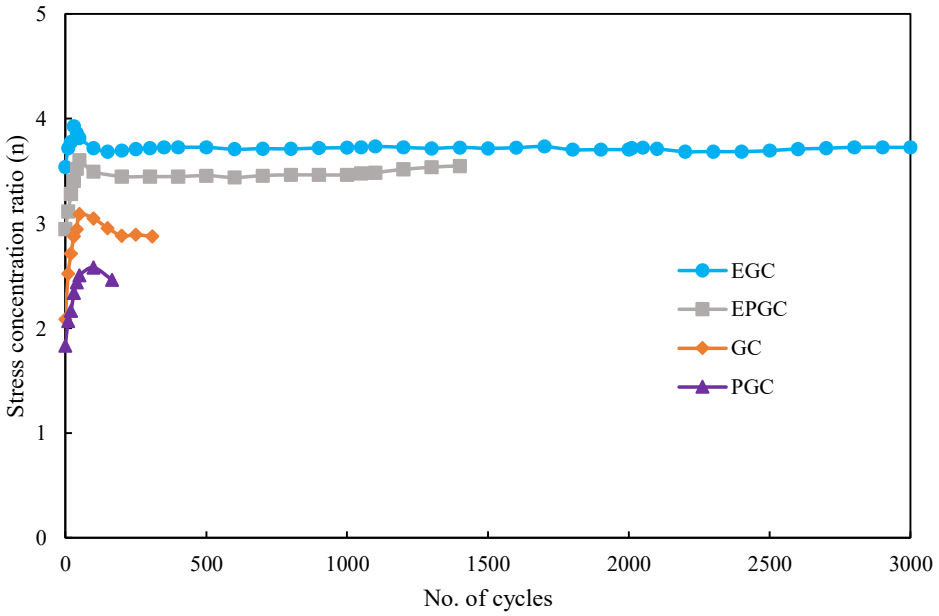

Fig. 5.10 Stress concentration ratio (n) of single-stage (stage 4) cyclic loading on model embankment.

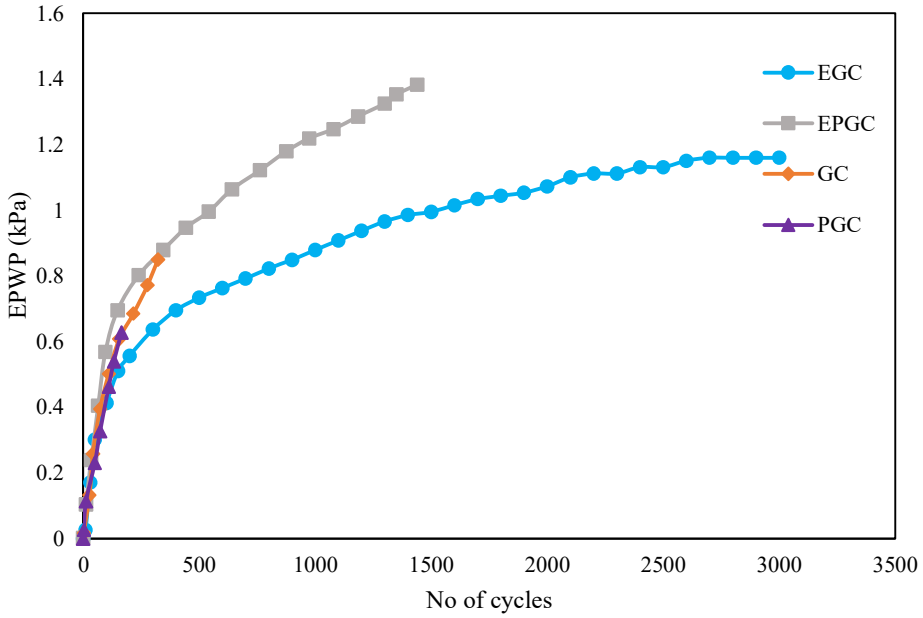

Fig. 5.11 Excess pore water pressure variation under single-stage cyclic loading.

The EPWP response obtained in the single-stage cyclic loading is shown in Fig. 5.11. It was observed that the EPWP response is similar for all the cases for the first 90-100 cycles. The EPWP buildup is steep for both PGC and GC, with 0.62 kPa and 0.85 kPa,

respectively, at 50 mm settlement. The EPWP trend for EPGC and EGC conditions shows an increasing behavior with a gradual approach toward a stable state at failure. The peak EPWP values of 1.38 kPa were observed for EPGC and 1.16 kPa for EGC at failure.

5.3.4 Embankment and column deformation behavior

The vertical settlement and lateral deformation of the granular columns were examined by physical exhumation of the soft cay bed. Soil was removed from one side of the test tank by opening the side plate after completing the loading tests. The deformed shape of the embankment and the granular columns is shown in Fig. 5.12. Fig. 5.12 (a) and (b) show the deformed model embankment. The punching of the soil under the footing plate is clearly observed in the figure. The deformation pattern of non-encased granular columns is seen in Fig. 5.12 (c) and (d) under floating and end-bearing conditions. The exhumation of soil to expose the deformed shape of columns for the non-encased columns was a little tricky as the columns were susceptible to breakage. The columns directly under the loading plate exhibited slight bulging near the top. This phenomenon is well-established in the literature. The deformed column behavior is observed for the encased columns under floating and end-bearing conditions in Fig. 5.12 (e) and (f). Floating columns exhibit punching under the footing plate, as shown in the figure. The end-bearing columns directly under the footing pate exhibit buckling along the length, possibly due to the hoop tension developed in the geosynthetic encasement under cyclic loading.

(a)

(b)

(c)

(d)

(e)

(f)

Fig. 5.12 Settlement response under cyclic loading of (a) embankment plan view, (b) embankment elevation, (c) GC FL, (d) GC EB, (e) EGC FL, (f) EGC EB.

5.3.5 Comparative settlement behavior under static, multistage cyclic, and single-stage cyclic loading

The settlement response of the GC-reinforced clay bed has been shown in Fig. 5.13 for floating and end-bearing column conditions to compare the behavior under cyclic and static loading. The cyclic loading-induced settlements were higher than those under static loading. The end-bearing GC under cyclic loading had a settlement of 29.9 mm at 56.9 kPa cyclic stress load, whereas that under-static loading was 25.25 mm. Also, at 73.1 kPa cyclic stress, end-bearing GC exhibited 24.34 % higher settlement. Higher settlement under cyclic loading is observed due to multiple cycles of the repeated stress applied to the soil. Similarly, a 17 % higher settlement was observed at a 56.9 kPa stress level for the floating GC.

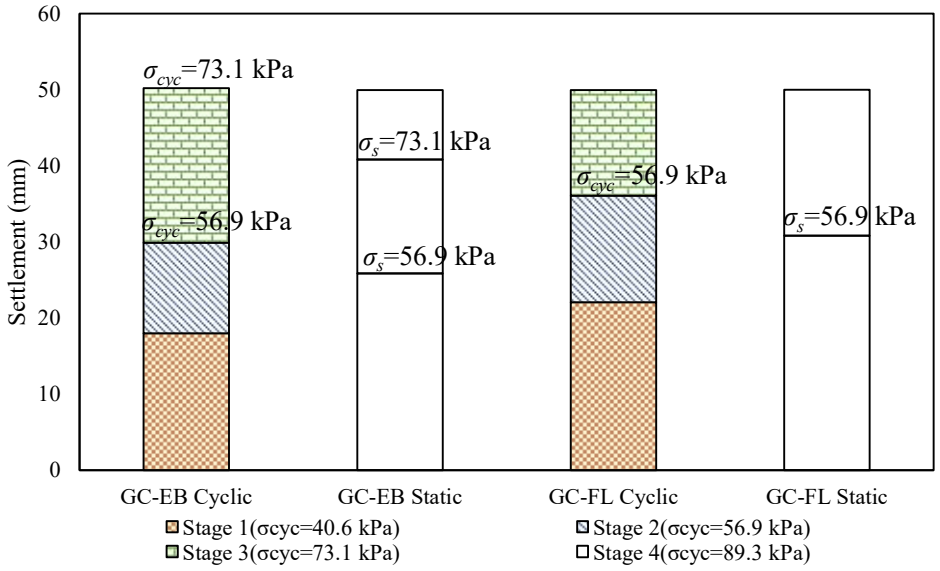

Fig. 5.13 Settlement response comparison for floating and end-bearing GC under cyclic and static loading.

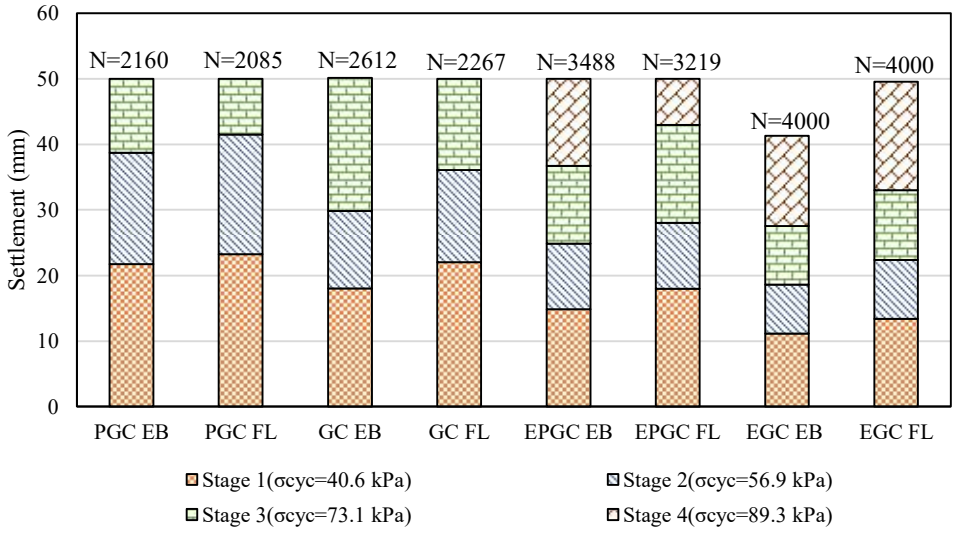

Fig. 5.14 Settlement response comparison for floating and end-bearing PGC, GC, EPGC, and EGC under cyclic loading.

The settlement response of the improved soil bed under multistage cyclic loading has been summarized in Fig. 5.14. It is evident from the plot that the end-bearing column performs better in settlement reduction under cyclic loading for all combinations of granular columns. Also, only the encased GC and PGC reinforced beds

had sustained all four stages of cyclic loading, with EGC undergoing 41.30 mm settlement at the end of 4000 cycles of staged loading.

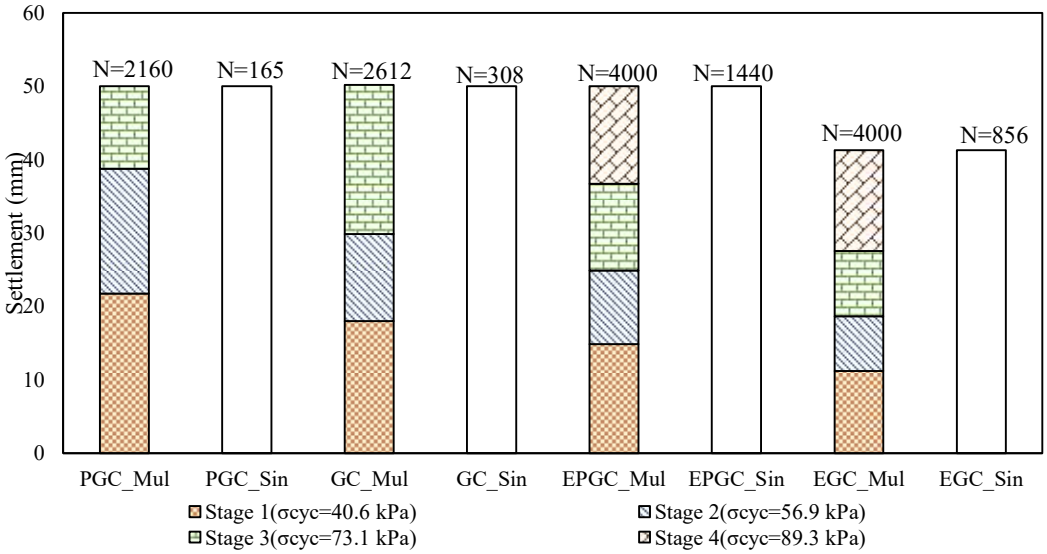

Fig. 5.15 Settlement response comparison of PGC, GC, EPGC, and EGC under single and multistage cyclic loading.

The comparative analysis of single and multistage cyclic loading was done as per the plot shown in Fig. 5.15. PGC underwent 50 mm settlement under 165 cycles of single-stage cyclic loading. GC exhibited better response under multistage cyclic loading. GC underwent a 50 mm settlement at 308 cycles of single-stage loading. For EPGC, the number of loading cycles is 1440 at 50 mm settlement, which is a reduction of 74 % in the number of cycles the embankment can handle. EGC underwent 41.3 mm settlement at 4000 cycles of multistage loading and 856 cycles of single-stage loading. The accumulated settlement of the improved bed reduces for PGC, GC, EPGC, and EGC, respectively. The settlement observed at the end of stage 1 cyclic loading was 21.74 mm, 18.01, 14.89 mm, and 11.17 mm, indicating a settlement reduction of 51.37 % for PGC and EGC under four-stage cyclic loading. This reduction was observed due to a stiffer response of EGC over PGC.

5.3.6 Environmental Assessment and Cost Estimation

The growing share of plastic materials in municipal waste is an environmental challenge. A report on plastic waste generation in India states that quite a bit of progress has been made in the recycling of plastics over the last decade (CPCB 2020).TERI (TERI 2021) estimates that 60% of the plastic waste generated in India is getting recycled. However, 31.5% of the total plastic waste is still mismanaged as litter in the streets, thrown into dumpsites, or burnt openly. The improper disposal of plastic waste, like open burning, emits harmful gases into the environment. Polypropylene (PP), Polyethylene terephthalate (PET), Polly vinyl chloride (PVC), Polyethylene (PE), and Acrylonitrile butadiene styrene (ABS) are the major contributors to the global plastic waste generation (Chu et al. 2022).

A comparison of the cost of the materials is presented, as shown in Table 5.3. The cost of the materials might differ from the values shown here as they are specific to a country and location. The involvement of governmental agencies in incentivizing the use of recycled plastics could substantially lower the cost by expanding the target area. The environmental impact of using recycled plastic granules as aggregates in construction activities was explored in the literature. Plastic waste is usually incinerated for proper disposal instead of open burning to contain air pollution (Chu et al. 2022). Studies have been done to estimate the emission during the incineration process of plastic wastes to quantify the environmental impact. The greenhouse gas (GHG) emissions during the incineration of plastic wastes are reported as CO_2 equivalent. In a recent study, the emissions from PE, PP, and PVC during incineration were reported to be 813, 812, and 381 kg eq C/t (Belmokaddem et al. 2020). The GHG emissions from ABS plastics in China were reported to be 144.84 kg eq C/t in 2017 (Chu et al. 2022). The use of recycled plastic as aggregates in the construction and transportation sector

will significantly contribute to solving problems associated with the disposal of plastic waste.

Table 5.3 Cost comparison of the materials used as aggregates in the granular columns.

Material	Cost ($/t)	References
Natural aggregates	26	(Saha et al. 2023a)
	25.5	(Ohemeng and Ekolu 2020)
Recycled Plastic granules	30	(Saha et al. 2023a)
	28-40	(Retail market rates in India)

5.4 Regulatory and economic challenges

The wide-scale commercial application of alternative materials as aggregates requires consistent research data that provides insights into their potential applications. Recent studies in this area could act as a catalyst for the interests of various stakeholders to expand research interests and explore future applications (Chu et al. 2022; Saleem et al. 2023). However, the lack of standardization in recycling waste plastic to produce granules may discourage its potential adaptability in field applications (Hamada et al. 2024). The production scale of recycled waste plastic aggregates is still low due to its limited application. As such, the present cost of production is a little higher than that of conventional materials, which could also be attributed to the lack of a regulatory framework guiding the use of recycled plastic in construction and other industries. Adopting proper quality control and standardizing the recycling process could help maintain the desired physical properties of the recycled plastic granules for greater applicability (Premathilaka et al. 2024).

5.5 Conclusions

Model tests on embankments constructed over soft clay beds improved with floating and end-bearing GCs or PGCs were conducted in this study. The performance of model embankments under static and cyclic loading was studied to simulate cyclic stresses induced in railway embankments. Based on the results obtained in this study, the following conclusions could be drawn:

8) A model embankment constructed over GC and a PGC-reinforced soft clay bed exhibited significant improvement in settlement response compared to an unreinforced clay bed. The vertical stress under static loading was improved by 71 % and 135 % for floating and end-bearing columns, respectively. Also, the EPWP is reduced by 1.70 times using end-bearing GC.
9) The variation of stress concentration for non-encased and encased granular columns was reported in this study. A stepwise decreasing trend of stress concentration was observed for GC and PGC improved soil bed over multistage cyclic loading. A contrasting stepwise increasing trend was reported for EGC and EPGC improved soil bed.
10) Excess pore water pressure variation over multistage cyclic loading has shown a successive increasing trend for granular column-improved soil beds. However, the rate of increment in EPWP is significantly reduced for EGC and EPGC reinforcement combinations.
11) The columns under the loading plate undergo bulging failure for GC and PGC configurations. The columns away from the footing are laterally displaced with no bulging deformation. Encased floating columns undergo punching under the footing with little lateral movement for columns away from the footing. End-bearing columns directly below the footing plate undergo slight buckling.

12) Using geosynthetic encasement with GCs and PGCs significantly reduces EPWP and improves stress concentration on the columns. Embankments constructed over EGC and EPGC-improved clay beds can better withstand cyclic and static loads.